www.czasopisma.pan.pl PAN www.journals.pan.pl
Opto-Electronics Review 27 (2019) 348–354

Contents lists available at ScienceDirect

Opto-Electronics Review

journal homepage: http://www.journals.elsevier.com/opto-electronics review

Review

Electrical and photoresponse characteristics of 8-(1*H*-indol-3-ylazo)-naphthalene-2-sulfonic acid/n-Si photodiode

I.T. Zedan[a,*], E.M. El-Menyawy[b], H.H. Nawar[c]

[a] *Renewable Energy Science and Engineering Department, Faculty of Postgraduate Studies for Advanced Sciences, Beni-Suef University, Beni-Suef 62511, Egypt*
[b] *Solid State Electronics Laboratory, Solid State Physics Department, Physics Research Division, National Research Centre, 33 El-Bohouth St., Dokki, Giza 12622, Egypt*
[c] *Department of Chemistry, Faculty of Education, Al-Zintan University, Libya*

ARTICLE INFO

Article history:
Received 15 September 2019
Accepted 29 November 2019
Available online 15 December 2019

Keywords:
Azo compounds
Conduction mechanism
Diode parameters
Photodiodes

ABSTRACT

In this paper, of primary interest is to synthesis 8-(1*H*-indol-3-ylazo)-naphthalene-2-sulfonic acid (INSA) and to evaluate the main parameters of Au/INSA/n-Si/Al diode in dark and under illumination. Different techniques are used for interpreting the proposed INSA chemical structure. The dark current-voltage measurements were achieved in the temperature range of 293–413 K. It is noticed that INSA films modify the interfacial barrier height of classical Au/n-Si junction. At low applied voltages, the I–V relation shows exponential behavior. The values ideality factor, n, and the barrier height, φ, are improved by heating. The abnormal trend of n and φ is discussed, and a homogenous barrier height of 1.45 *eV* is evaluated. The series resistance is also calculated using Norde's function and it changes inversely with temperature. The space charge limited current ruled with exponential trap distribution dominates at relatively high potentials, trap concentration and carriers mobility are extracted. The reverse current of the diode has illumination intensity dependence with a good photosensitivity indicating that the device is promising for photodiode applications.

Contents

1. Introduction

A considerable attention has intensively been focused to the field of organic semiconductors and their devices for advanced technological applications. Organic semiconductors are cheap materials, lightweight and biocompatible compared with expensive inorganic semiconductors, and they have worthy motivating properties. Special interest has been dedicated to the building of organic-based photodiodes [1]. The photodiodes are classical diodes which are sensitive to light detection in which the magnitude of the created photocurrent changes with the incident light beams intensities. They are one of the most important photo electronic devices which used in many important fields; photoconductors, compact disc players, detectors for computed tomography, organic photovoltaic devices, lighting regulation, and photo multiplier tubes [1–3].

* Corresponding author.
E-mail address: islam.taha@psas.bsu.edu.eg (I.T. Zedan).

https://doi.org/10.1016/j.opelre.2019.11.006
1230-3402/

The organic material under investigation named as 8-(1*H*-indol-3-ylazo)-naphthalene-2-sulfonic acid (INSA) is a typical aromatic azo compound with molecular formula of $C_{18}H_{13}N_3O_3S$. The main features of azo dyes as conjugated molecules have been shown in the light-induced photo process and many applications in thin film electronic devices. Azo dyes are extensively studied due to their superior characteristics such as low cost and tunable properties [4]. Motiei *et al.* [5] have been used azo dyes in optical switching devices. Besides, Westphal *et al.* [6] synthesized discotic azo for electro-optical devices. Azo dyes with push-pull character have successfully been applied in dye-sensitized solar cell [7] with reasonable photo-electrical conversion efficiency. Güllü *et al.* [3] have been utilized orange G (OG), as an aromatic azo compound, in the diode structure of Al/OG/n-Si/AuSb and pointed out that it can help to provide a modified barrier height, φ, value of 0.86 *eV*, but the value of ideality factor, *n*, was too high as it was estimated as 4.35. They explained this departure of *n* value from ideal value to highly resistive OG film and the presence of thin native SiO_2 on the surface of the n-Si. INSA compound is nearly similar in molecular structure to OG with the modification in the aromatic moiety resulting in more π electrons which contributes to more delocalization of electrons and subsequently more stability.

It is well known that the introduction of organic films, as inter-layer between metals and inorganic semiconductors, modifies performance of the classical diodes due to the interfacial properties [8–11]. These devices are more preferred than conventional metal/inorganic diodes due to their fascinating properties [9,12–14]. In this work, it is inspired to synthesize of INSA compound and use it in the heterojunction structure of Au/INSA/n-Si/Al. The full dark electrical characterization of the fabricated device is explored. The effect of illumination with different light intensities on the *I-V* curves is also studied.

2. Experimental procedures

2.1. Synthesis of INSA compound

8-(1*H*-indol-3-ylazo)-naphthalene-2-sulfonic acid (INSA) was prepared by dissolving 0.8 g of anhydrous sodium carbonate in 15 ml H_2O. Then, 1 g of 8-aminonaphthalene-2-sulfonic acid was added to the solution, and then the mixture was heated aiming for complete dissolving. Then, the solution was cooled to room temperature and 0.4 g of sodium nitrite under magnetic stirring. After complete dissolving, the solution exhibits pale yellow color. Then the solution was poured into a 200 ml Erlenmeyer flask containing 3 ml of H_2O, 1.5 ml of concentrated HCl (12 M) and 5 g of ice or enough to just cover the bottom of the flask. The diazonium salt of 8- aminonaphthalene-2-sulfonic acid was then added to the ethanolic solution of indole at 0°C. The mixture was kept in an ice bath for another 15 min to permit the coupling reaction completion. The crude product was collected by suction filtration, washed, dried and re-crystalized to obtain INSA dark gray crystals in yield of 80 %, m.p. > 400 °C. The chemical reaction for obtaining INSA compound is donated in Scheme 1. IR (ν_{max}/cm^{-1}): 3380, 3303 (—OH, —NH), 3116, 3064, 2924, 2862 (C—H stretching), 1608 (Ar. ring). ^{1}H NMR (DMSO–d_6) (δ, ppm): 2.49 (s, 1H, S—OH), 8.40–8.79 (m, 3H, naphthalene protons), 7.00–8.20 (m, 3H, naphthalene protons), 7.10–7.64 (m, 4H, indole protons), 9.16 (s, 1H, N—H). MS (FAB): *m/z* = 351.07; Elemental analysis: Calcd. $C_{13}H_{13}N_3OO_3S$: C, 61.53; H, 3.73; N, 11.96. Found C, 61.01; H, 3.75; N, 11.95.

2.2. Diode fabrication

Si wafers with phosphor dopant (n-Si) were used for diodes fabrication. The wafer thickness and resistivity are of 0.4 mm and 10 Ω.cm, respectively; these wafers are oriented at (100) direction. Firstly, the wafers were cleaned according to the procedures reported by us in Ref. 11 before the deposition of the organic layer on n-Si. An ohmic contact of Al was deposited on the back of n-Si wafers. The wafers coated with Al were heated at 550 °C under Ar flow for 1 h. Then, organic film with a thickness of 50 nm was deposited on the front surface of n-Si. After that, Au electrode was made on the top of organic layer to obtain Au/INSA/n-Si/Al structure with area of 0.6 cm^2.

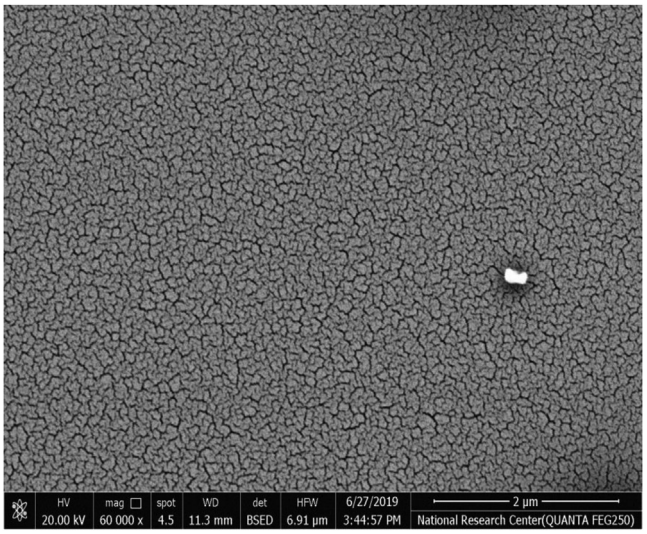

Fig. 1. FESEM image of INSA film.

2.3. Instrumentation

All evaporation processes were done under vacuum pressure of 10^{-3} Pa with aid of coating unit (model E306 A, Edwards Co.). The film thickness was controlled by quartz crystal thickness monitor with a rate of 1 Å/s. Nuclear magnetic resonance (^{1}H NMR) spectra were measured using varian Mercury-vx-300 NMR spectrometer using deuterated dimethyl sulfoxide (DMSO-d_6) as solvent. Fourier transforms infrared (FTIR) spectra were verified on ATI Mattson infrared spectrophotometer in spectral range 4000–400 cm^1. The composition of C, H and N elements of INSA powder was determined using PERKIN–ELMER 2400 CHN elemental analyzer.

The surface morphology of INSA films was investigated by scanning electron microscope (SEM) (Quanta TEG 250). The source meter electrometer (Keithly type 2635A) was used for measuring the current-voltage (*I-V*) data of the device at different temperatures in the range of 293–410 K. The temperature was measured using NiCr-NiAl thermocouple. The illumination was achieved with 100 W filament lamps. Luxmeter (model Lx-102 light meter) was used for estimating light intensity.

3. Results and discussions

3.1. Morphology of INSA films

The surface morphology image of INSA is illustrated in Fig. 1. The image clarifies the rough nature of INSA surface with amorphous structure. The film surface contains granular-shaped distributed particles together with the presence of cracks.

3.2. Electrical characterization

I–V curves of Au/INSA/n-Si/Al heterojunction measured in dark oven at different temperatures (293–413 K) are depicted in Fig. 2.

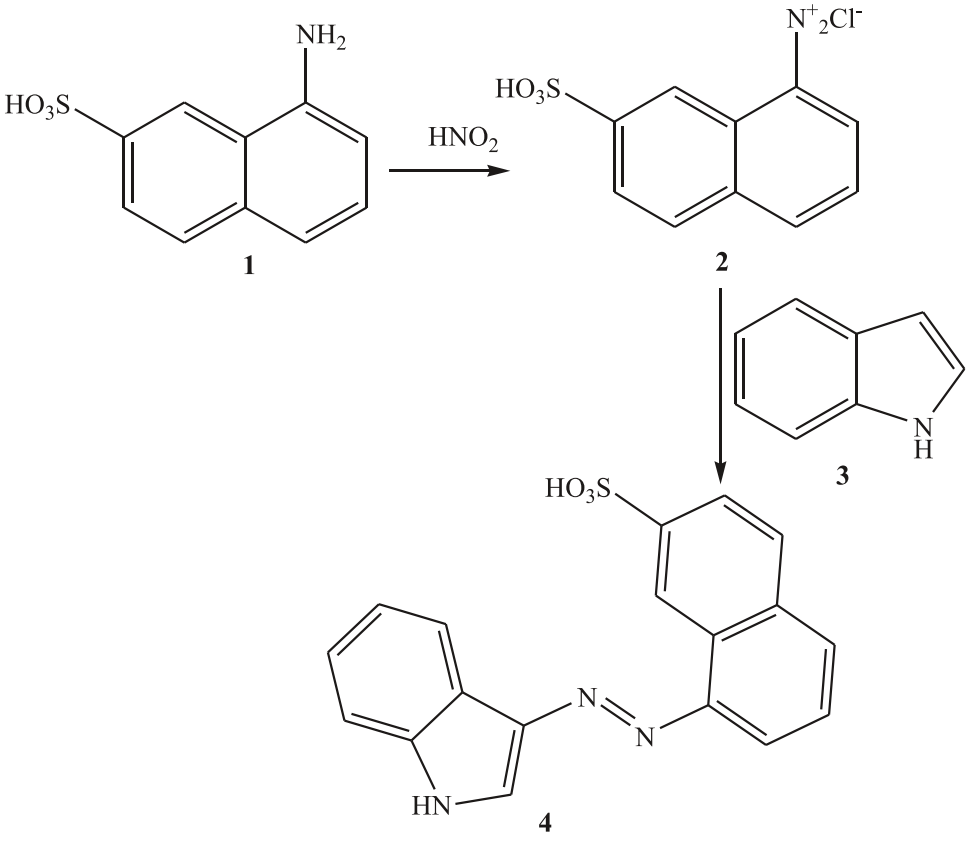

Scheme 1. Chemical reaction for obtaining INSA compound.

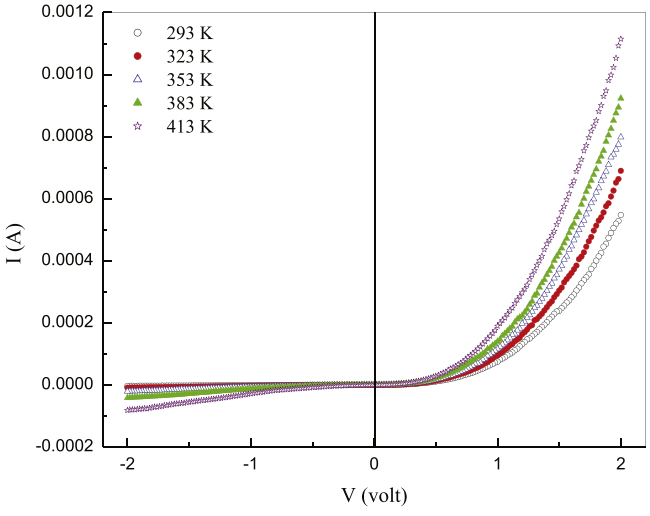

Fig. 2. *I-V-T* curves of Au/INSA/n-Si/Al heterojunction.

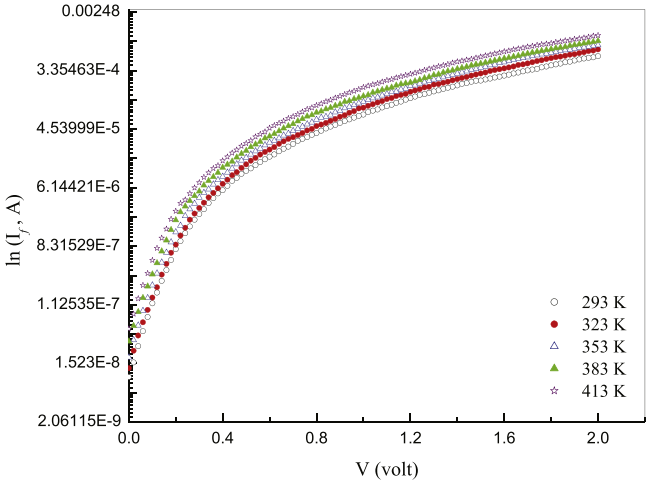

Fig. 3. The relation between lnI_f and V for Au/INSA/n-Si/Al heterojunction.

The curves provide the conventional behavior of diodes with a moderately room temperature rectification ratio of 88 calculated at ±1.5 V. The current increases with increasing temperature in both forward and reverse directions.

Figure 3 shows the relation between $\ln I_f$ and V in the voltage range $0 \le V \le 2$. The relation can generally be divided into two regions: (i) at voltage range $0 \le V \le 0.22$ and (ii) at voltage range $0.22 < V \le 2$. At first region, the relation yields straight line behavior with linearity dependence on the temperature and at the second region, there is a deviation from this behavior, which can be ascribed to the effect of diode series resistance, R_s.

The exponential increasing of current can be explained according to thermionic emission mechanism:

$$I = AA^*T^2e^{-B\varphi}\left[e^{(BV/n)} - 1\right]. \quad (1)$$

where, A is the diode area, A^* is the Richardson constant (112 A cm^{-2} K^{-2} for n-Si [15]), T is the temperature in Kelvin, $B = q/k_BT$, q is the elementary charge and k_B is the Boltzmann constant. Values of n and φ at different temperatures are calculated from straight-lines slope and their intercepts with I axis. Values of n and φ are found to be 1.87 and 0.86, respectively, at room temperature (293 K). So, it can be observed that φ value of Au/n-Si junction (0.79 *eV* [16]) is modified due to the presence of INSA interlayer. Besides, the

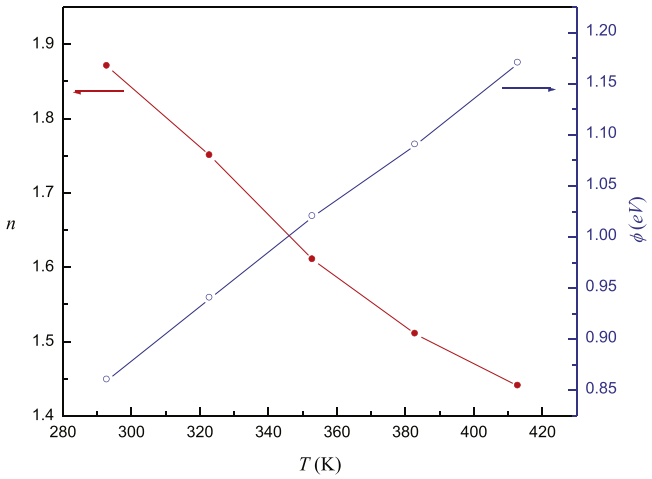

Fig. 4. Dependence of barrier height and ideality factor on temperature.

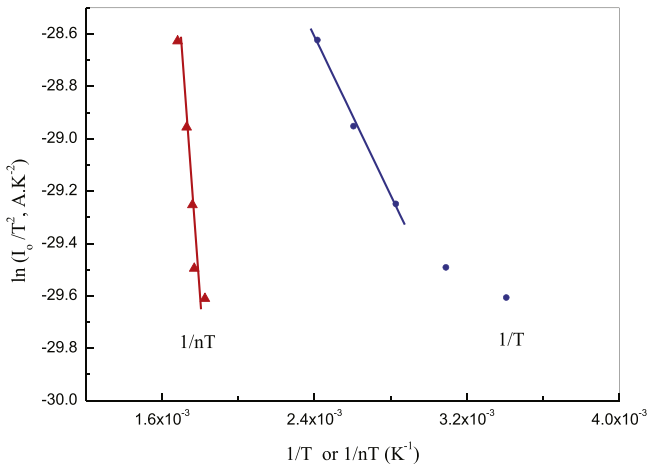

Fig. 5. Richardson plots for Au/INSA/n-Si/Al diode.

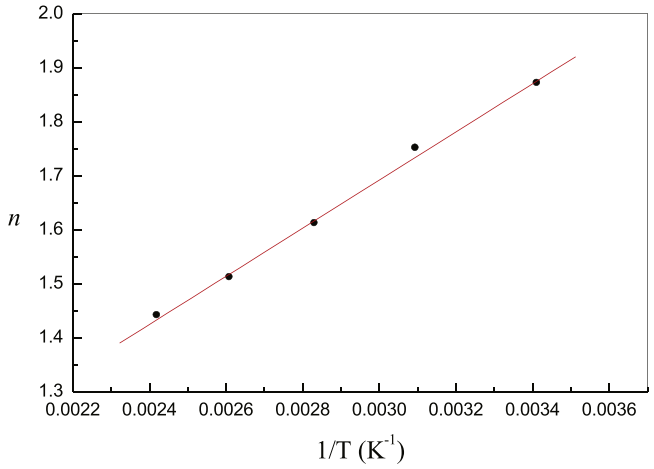

Fig. 6. Variation of n with inverse of temperature.

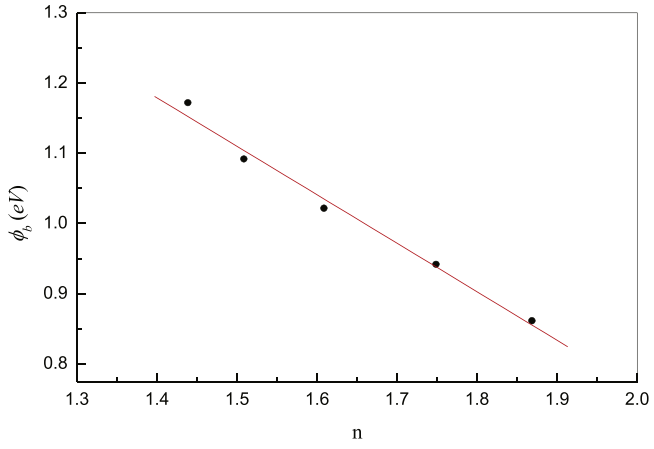

Fig. 7. The barrier height versus ideality factor.

obtained value of n is an indicator of non-ideal device. Although n value is still greater than unity, it is better than that obtained for OG interlayer between Au and n-Si [3]. Several authors have been investigated the effect of the organic interlayer on the performance of n-Si [10,11,17,18]. Takanashi *et al.* [17] estimated the values of φ and n of 0.75 *eV* and 3.3, respectively, for Au/α-sexithiophene/n–Si heterojunction using Cheung method. The φ value is lower than the classical value of Au/n-Si, in which they attributed the high value of n to the generation of an interfacial layer at the heterojunction. Çulcu *et al.* [18] studied the *I-V* characteristics of Au/poly (linoleic acid)-g-poly(methyl methacrylate)/n-Si diode and expressed the values of φ and n as 0.87 *eV* and 3.3, respectively. These results indicate that the value of φ can be decreased or increased by the presence of organic interlayers. From the temperature dependence of n and φ (shown in Fig. 4), it can observed that the n value decreases, while φ value increases with increasing temperature due to an inhomogeneity at interface between INSA layer and n-Si.

Using thermionic emission theory, Richardson relation can be written as:

$$\ln\left(\frac{I_o}{T^2}\right) = (\ln A^*) - \left(\frac{q\emptyset}{k_B}\right)\left(\frac{1}{T}\right), \tag{2}$$

where, I_o refers to the reverse saturation current. Figure 5 depicts Richardson plots ($ln(I_o/T^2)$ *vs.* $1/T$ and $1/nT$) in the temperature range from 293 to 413 K. According to thermionic emission theory, the relation between $ln(I_o/T^2)$ and $1/T$ should be fitted well as a straight line relationship. However, it can be a fitted for only three points. This fitting yields the values of A^* and φ as 2.31×10^{-11} A cm^{-2} K^{-2} and 0.13 *eV*, respectively. The deviation from the linearity and the low values of A^* and φ is caused by the temperature dependence of n and φ together with the inhomogeneity in barrier height [19]. Similar results were found by several authors [20–22]. By considering the tunneling conduction, the Richardson relation can be modified by the introduction of the ideality factor. Then, the relation between $ln(I_o/T^2)$ and $1/nT$ should be straight line which is verified as shown in Fig. 5. The straight line fitting yields the values of A^* and φ as 1.26×10^{-7} A cm^{-2} K^{-2} and 0.63 *eV*, respectively. Again, the A^* value is much smaller than the supposed theoretical value and the value of φ is lower than the expected value as compared with the calculated values from the *I-V* using the theoretical value of A^* which can be understand in terms of the inhomogeneity in barrier heights [26,23]. Generally, at the diode interface, the T_0 effect is ascribed by inversely proportional of n with temperature. The variation of the n with temperature is expressed as [24]:

$$n = 1 + \left(\frac{T_o}{T}\right), \tag{3}$$

where, T_o is constant. Figure 6 depicts the variations of n *vs.* the reciprocal temperature. The relation is linear which is in accordance with Eq. (3). Accordingly, the observed behavior can be explained in terms of inhomogeneity of barriers. The T_o value is estimated as 445 K.

The relation between φ and n values for Au/INSA/n-Si/Al heterojunction is depicted in Fig. 7. According to Schmitsdorf *et al.* [25] and based on used Tung's theoretical approach, the homogenous bar-

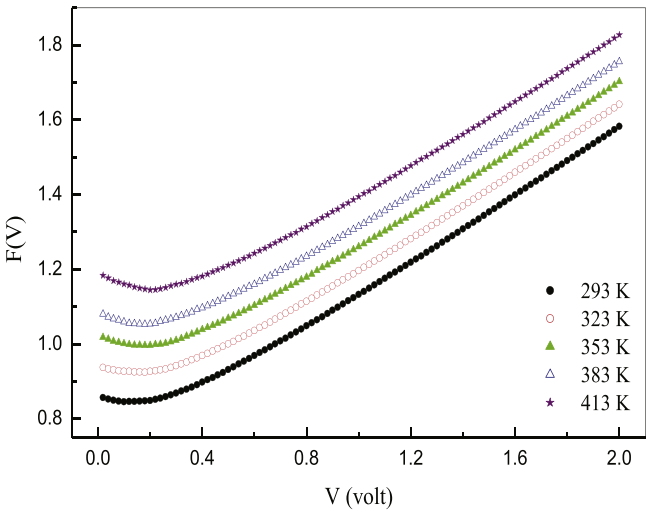

Fig. 8. Norde's function-voltage relation for the Au/INSA/n-Si/Al heterojunction.

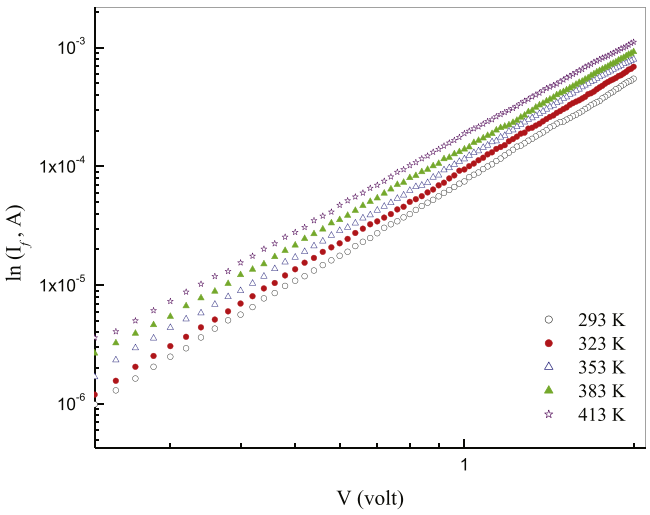

Fig. 9. Relation between lnI_f and ln$V$ at relatively high voltages.

Table 1
Diode parameters at different temperatures.

T (K)	I-V method		Norde's function	
	n	$\varphi(eV)$	R_s(kΩ)	$\varphi(eV)$
293	1.87	0.86	27.841	0.87
323	1.75	0.94	10.473	0.987
353	1.61	1.02	8.861	1.065
383	1.51	1.09	8.519	1.11
413	1.44	1.17	7.227	1.21

rier height of diodes can be estimated from the relation between the φ and n by the extrapolation of the straight line fitting of the data towards the φ axis at unity value of n. The experimental data are fitted as a straight line relation with a homogeneous φ value of 1.45 eV.

In order to estimate the value of R_s, Norde's function is calculated using classical expression [26]. Figure 8 depicts Norde's function against the potential for the Au/INSA/n-Si/Al heterojunction. From the minimum values of Norde's function $F(V_{min})$ appeared at low voltages and its related current $I(V_{min})$, the R_s and φ are calculated using Norde's method and are given in Table 1. The charge carriers are activated with increasing temperature, consequently the value of R_s is improved. The values of φ are in good agreement with the obtained from I-V characteristics. The room temperature value of φ is comparable with that for OG [3].

At relatively high voltage more than 0.22 up to 2 V, the relation between lnI_f *vs.* ln$V$, at different temperatures, is found to be linear as illustrated in Fig. 9. The slope of the straight line fitting is estimated as 2.84 at 293 K and decreases slightly with temperature down to 2.66 at 413 K. These results validate the relation of $I \alpha V^m$, with exponent m greater than 2. This power law indicates that the space charge limited current (SCLC) controlled by exponential trap distribution inside the forbidden gap is the operating conduction mechanism for charge carriers in the considered voltage range This exponential trap distribution explained by a temperature parameter T_t which is an indicator of defects loss. According to Lampert equation, the current density is given by [27]:

$$J_{SCLC} = \mathrm{e}\,\mu N_v \left(\frac{\varepsilon}{qP_o k_B T}\right)\left(\frac{V^{l+1}}{d^{2l+1}}\right), \tag{4}$$

where, μ refers to the hole mobility, ε is the INSA permittivity, N_v is the density of states at the valence band edge (VBE), P_o is the

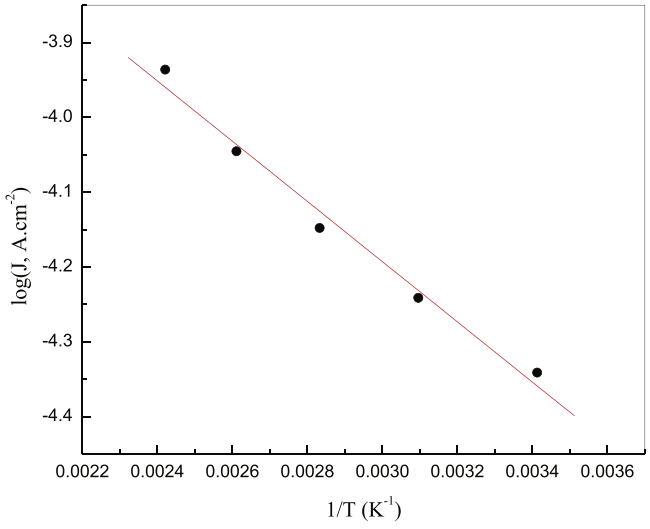

Fig. 10. The relation between log$J$ and $1/T$ at 0.7 V.

trap density per unit energy range at the VBE, and l=T_t /T. The total concentration of traps is given by:

$$N_t = P_o k_B T_t. \tag{5}$$

The temperature parameter T_t is determined as 539 K. Figure 10 depicts the relation between log$J$ *vs.* $1/T$ at voltage 0.7 V. The relation gives straight line with a slope of S and an intercept of C. These values are expressed by [10]:

$$S = T_t \log\left(\frac{\varepsilon V}{ed^2 N_t}\right). \tag{6}$$

$$C = \log\left(\frac{e\mu N_v V}{d}\right). \tag{7}$$

Substituting N_v=10^{27} m^{-3} for organic materials [28], analysis gives the values of N_t and μ as 1.32×10^{23} m^{-3} and 2.55×10^{-12} $cm^2.V^{-1}.s^{-1}$, respectively. The low value of carrier mobility can be correlated with relatively high value of N_t which is also responsible for high R_s value. The value of N_t is in the same order of many of organic materials [29–31].

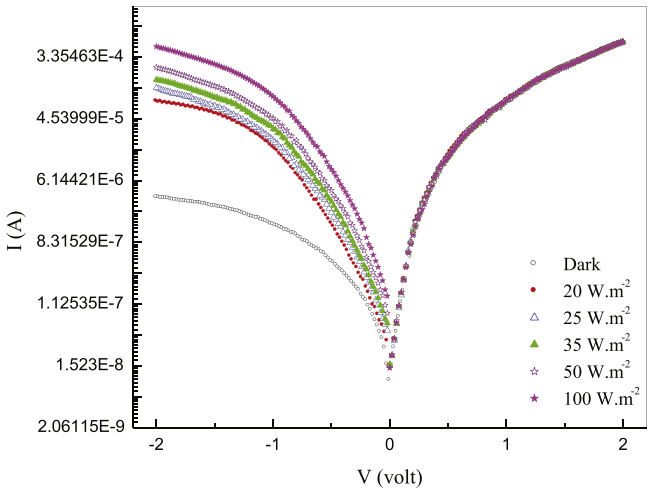

Fig. 11. Effect of illumination on the *I–V* curve of Au/INSA/n-Si/Al heterojunction.

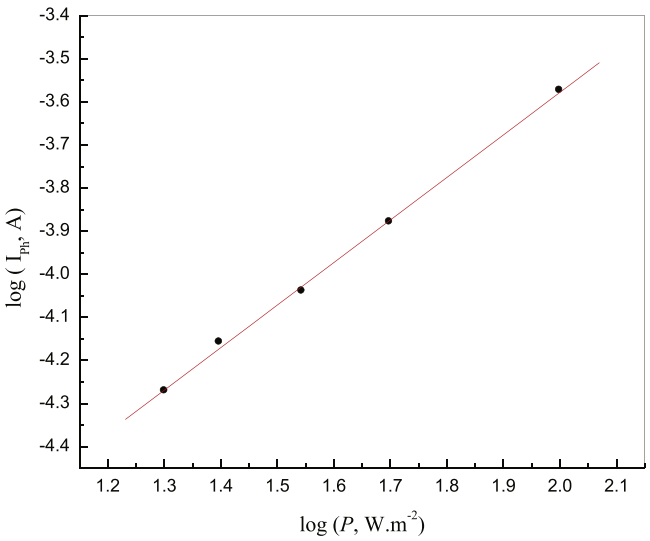

Fig. 12. Double logarithmic I_{Ph}-P relation for Au/INSA/n-Si/Al photodiode.

3.3. *Photoresponse characteristics*

The photoresponse curves of Au/INSA/n-Si/Al diode measured as a function of light intensity (20, 25, 35, 50 and 100 W/m^2) is depicted in Fig. 11. As a result of exposure to the light, the reverse current increases significantly with increasing light intensities. This means that, as a result of illumination, some of created electron-hole pairs are swept by the applied potential resulting in an increment of the current. This behavior indicates that the device holds enough justification in photodiode applications. The current of the Au/INSA/n-Si/Al photodiode determined at −1.5 V, increases from the dark value of 2.7×16^{-6} to 2.67×10^{-4} A as a result of illumination with light intensity of 100 W/m^2. Usually, not all of created electron-hole pairs contribute in the photocurrent enhancement due to possible recombination. In order to shed the light on the mechanism of this recombination, the variation of the photocurrent with the intensity of the impinging light should be investigated. In general, the photocurrent, I_{Ph}, is proportional to the illumination intensity, P, as:

$$I_{Ph} = \alpha P^{\gamma}, \tag{8}$$

where, α is a scaling current constant. The power law exponent factor γ depends on the nature of the medium and its value highlights the photo-conducting mechanism type for the fabricated photodiodes. The recombination process is adjustable by the γ value, since it has a value of unity and half in case of monomolecular recombination and bimolecular recombination, respectively. The value of γ for the fabricated photodiode is calculated as 0.99 from the slope of the relation between logI_{Ph} and log$P$ at -1.5 *V* depicted in Fig. 12. This value is closed to unity; which refers to monomolecular recombination mechanism. For further analysis concerning the effect of illumination on the diode photocurrent, the value of the photosensitivity, S, which is a measure of the current gain due to illumination, is calculated according to the expression [32]:

$$S = \left(\frac{I_{Ph} - I_{Dark}}{I_{Dark}}\right) \times 100\%, \tag{9}$$

where, I_{Dark} is the dark current. The value of S is estimated as 18.84, 24.74, 32.78, 47.89 and 97.89 % at illumination intensity of 20, 25, 35, 50 and 100 W/m^2, respectively. This indicates that the photosensitivity increases with increasing light intensity, which is in accordance with the photodiode behavior.

4. Conclusions

In conclusion, we have synthesized 8-(1*H*-Indol-3-ylazo)-naphthalene-2-sulfonic acid (INSA) compound and it is used to fabricate Au/INSA/n-Si/Al heterojunction. The diode *I-V* curves give a good rectifying behavior. The electrical analysis is achieved based on thermionic emission, tunneling mechanisms and space charge mechanisms. Values of n and φ are determined as 1.87 and 0.86 *eV*, respectively, at room temperature revealing that INSA films modify the interfacial barrier height of traditional Au/Si Schottky diode. The behavior of the ideality factor and barriers height is correlated to the inhomogeneity of the barrier heights in which the T_o effect is applicable. The series resistance extracted using Norde's function decreases with increasing temperatures. SCLC dominated by exponential trap distribution is dominant at relatively high voltage, the carriers mobility and trap concentration are determined as 2.55×10^{-12} cm^2.V^{-1}.s^{-1} and 1.32×10^{23} m^{-3}, respectively. Although the diode has low value of carriers mobility, the current in reverse direction is enhanced under applying different magnitude of illumination representing that the device under investigation can be used as photodiode.

References

[1] H.M. Zeyada, M.M. El-Nahass, M.M. El-Shabaan, Photovoltaic properties of the 4H-pyrano[3,2-c]quinoline derivatives and their applications in organic–inorganic photodiode fabrication, Synth. Met. 220 (2016) 102.
[2] T. Kilicoglu_, M.E. Aydin, Y.S. Ocak, The determination of the interface state density distribution of the Al/methyl red/p-Si Schottky barrier diode by using a capacitance method, Physica B 388 (2007) 244.
[3] O. Gullu, S. Aydogan, A. Turut, Fabrication and electrical characteristics of Schottky diode based on organic material, Microelectron. Eng. 85 (2008) 1647.
[4] A. Bafana, S.S. Devi, T. Chakrabarti, Azo dyes: past, present and the future, Environ. Rev. 19 (1) (2011) 350.
[5] H. Motiei, A. Jafari, R. Naderali, Third-order nonlinear optical properties of organic azo dyes by using strength of nonlinearity parameter and Z-scan technique, Opt. Laser Technol. 88 (2017) 68.
[6] E. Westphal, I.H. Bechtold, H. Gallardo, Synthesis and optical/thermal behavior of new azo photoisomerizable discotic liquid crystals, Macromolecules 43 (2010) 1319.
[7] B. Basheer, T.M. Robert, K.P. Vijayalakshmi, D. Mathew, Solar cells sensitised by push–pull azo dyes: dependence of photovoltaic performance on electronic structure, geometry and conformation of the sensitizer, Int. J. Ambient Energy 39-5 (2018) 433.
[8] A.R.V. Roberts, D.A. Evans, Modification of GaAs Schottky diodes by thin organic interlayers, Appl. Phys. Lett. 86 (2005) 072105.
[9] M. Lonergan, Charge transport at conjugated polymer-inorganic semiconductor and conjugated polymer-metal interfaces, Annu. Rev. Phys. Chem. 55 (2004) 257.

[10] E.M. El-Menyawy, Electrical and photovoltaic properties of Gaussian distributed inhomogeneous barrier based on tris (8-hydroxyquinoline) indium/p-Si interface, Mater. Sci. Semicond. Process. 32 (2015) 145.
[11] I.T. Zedan, N.A. El-Ghamaz, E.M. El-Menyawy, Geometrical and crystal structures, optical absorption and device characterization of N-(5-{[antipyrinyl-hydrazono]-cyanomethyl}-[1,3,4]thiadiazol-2-yl)-benzamide, Mater. Sci. Semicond. Process. 39 (2015) 408.
[12] I.T. Zedan, F.M.A. El-Taweel, R.A.N. Abu El-Enein, H.H. Nawar, E.M. El-Menyawy, Optical properties and junction characteristics of 6-(5-Bromothiohen-2-yl)-2,3-Dihydro-1-Methyl-3-Oxo-2-Phenyl-1H-Pyrazolo[4,3-b]Pyridine-5-Carbonitrile films, J. Electron. Mater. 45 (11) (2016) 5928.
[13] E.M. El-Menyawy, I.T. Zedan, Optical properties and device characteristics of 2-(antipyrin-4-ylhydrazono)-2-(4-nitrophenyl)acetonitrile thin films for photodiode applications, Spectrochim. Acta A. 137 (2015) 810.
[14] I.T. Zedan, E.M. El-Menyawy, A.M. Mansour, Physical characterizations of 3-(4-methyl piperazinylimino methyl)rifampicin films for photodiode applications, Silicon 11–3 (2019) 1693.
[15] E. Hökelek, G.Y. Robinson, A comparison of Pd schottky contacts on InP, GaAs and Si, Solid. Electron. 24 (1981) 99.
[16] S. Mahato, J. Puigdollers, Temperature dependent current-voltage characteristics of Au/n-Si Schottky barrier diodes and the effect of transition metal oxides as an interface layer, Physica B 530 (2018) 327.
[17] Y. Takanashi, N. Oyama, K. Momiyama, Y. Kimura, M. Niwano, F. Hirose, Alpha-sexthiophene/n− Si heterojunction diodes and solar cells investigated by I–V and C–V measurements, Synth. Met. 161 (2012) 2792.
[18] H. Çulcu, M. Gökçena, A. Allı, S. Allı, Current-voltage characteristics of Au/PLiMMA/n-Si diode under ultraviolet irradiation, J. Phys. Chem. Solids 103 (2017) 197–200.
[19] M.K. Hudait, P. Venkateswarlu, S.B. Krupanidhi, Electrical transport characteristics of Au/n-GaAs Schottky diodes on n-Ge at low temperatures, Solid. Electron. 45 (2001) 133.
[20] N. Tugluoglu, S. Karadeniz, M. Sahin, H. Safak, Temperature dependence of current–voltage characteristics of Ag/p-SnSe Schottky diodes, Appl. Surf. Sci. 233 (2004) 320.
[21] O.F. Yuksel, N. Tugluoglu, B. Gulveren, H. Safak, M. Kus, Electrical properties of Au/perylene-monoimide/p-Si schottky diode, J. Alloys. Compd. 577 (2013) 30.
[22] S. Karatas, S. Altındal, A. Turut, A. Ozmen, Temperature dependence of characteristic parameters of the H-terminated Sn/p-Si(100) Schottky contacts, Appl. Surf. Sci. 217 (2003) 250.
[23] B. Abay, G. Cankaya, H.S. Guder, H. Efeoglu, Y.K. Yogurtcu, Barrier characteristics of Cd/p-GaTe Schottky diodes based on I–V–T measurements, Semicond. Sci. Tech. 18 (2002) 75.
[24] M.K. Hudait, P. Venkateswarlu, S.B. Krupanidhi, Electrical transport characteristics of Au/n-GaAs Schottky diodes on n-Ge at low temperatures, Solid-State Electron. 45 (2001) 133.
[25] R.F. Schmitsdorf, T.U. Kampen, W. Monch, Correlation between barrier height and interface structure of Ag/Si(111) schottky contacts, Surf. Sci. 324 (1995) 249.
[26] H. Norde, A modified forward I-V plot for Schottky diodes with high series resistance, J. Appl. Phys. 50 (1979) 5052.
[27] M.A. Lampert, Volume-controlled current injection in insulators, Rep. Prog. Phys. 27 (1964) 329.
[28] A. Sussman, Space charge limited currents in copper phthalocyanine thin films, J. Appl. Phys. 38 (1967) 2738.
[29] A.K. Hassan, R.D. Gould, The electrical properties of copper phthalocyanine thin films using indium electrodes, J. Phys. D 22 (1989) 1162.
[30] A. Ahmed, R.A. Collins, Ohmic and space charge limited conduction in lead phthalocyanine thin films, Phys. Status Solidi A 123 (1991) 201.
[31] E.M. El-Menyawy, A.M. Mansour, N.A. El-Ghamaz, S.A. El-Khodary, Electrical conduction mechanisms and thermal properties of 2-(2, 3-dihydro-1,5-dimethyl-3-oxo-2-phenyl-1H-pyrazol-4-ylimino)-2-(4-nitrophenyl)acetonitrile, Physica B 413 (2013) 31.
[32] J.J. Hassan, M.A. Mahdi, S.J. Kasim, N.M. Ahmed, H. Abu Hassan, Z. Hassan, High sensitivity and fast response and recovery times in a ZnO nanorod array/p-Si self-powered ultraviolet detector, Appl. Phys. Lett. 101 (2012) 261108.